Title: Sensitive *in vivo* Visualization of Breast Cancer Using Ratiometric Protease-activatable Fluorescent Cancer Imaging Agent, AVB-620

Supplementary Materials:

A.

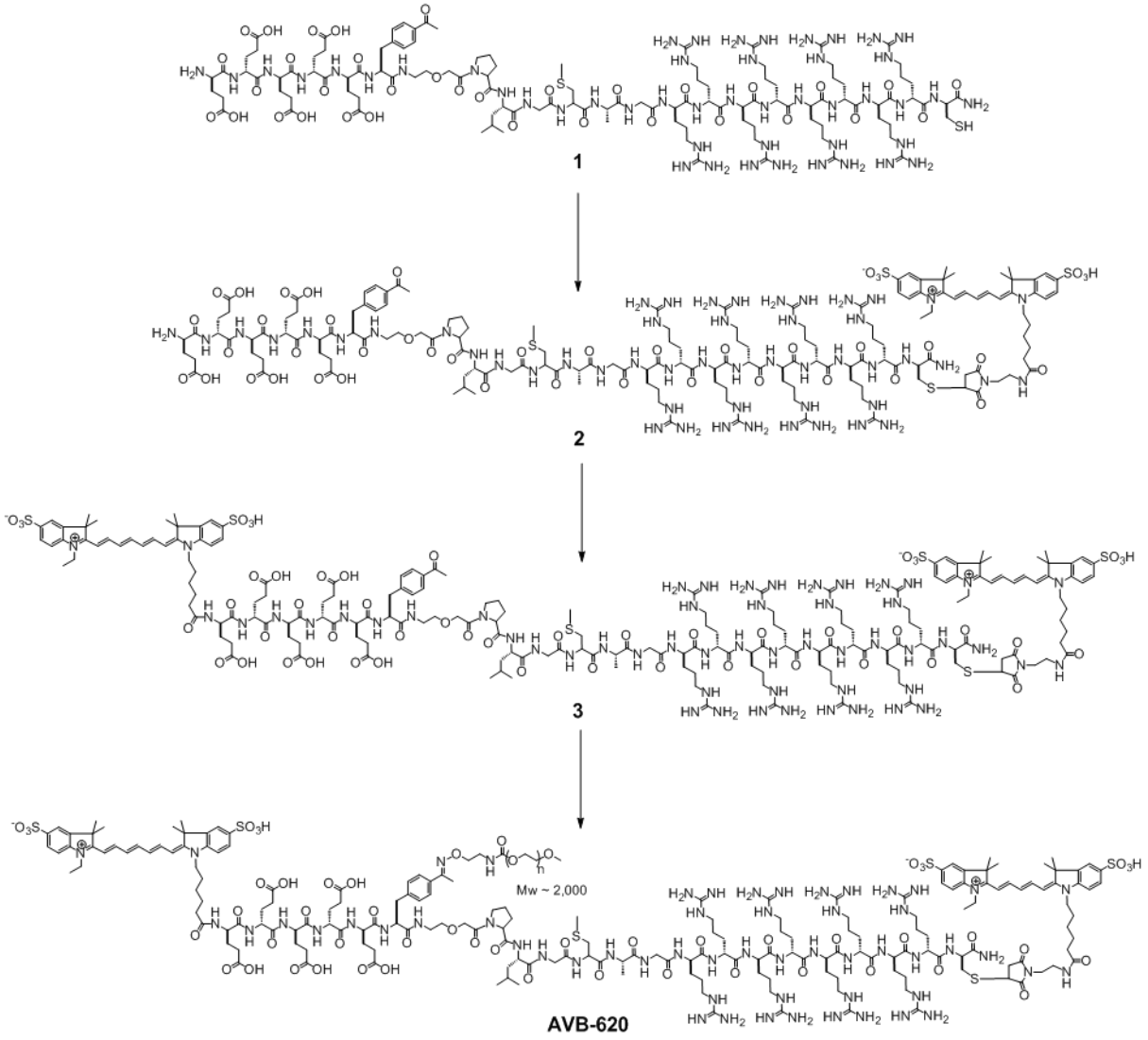

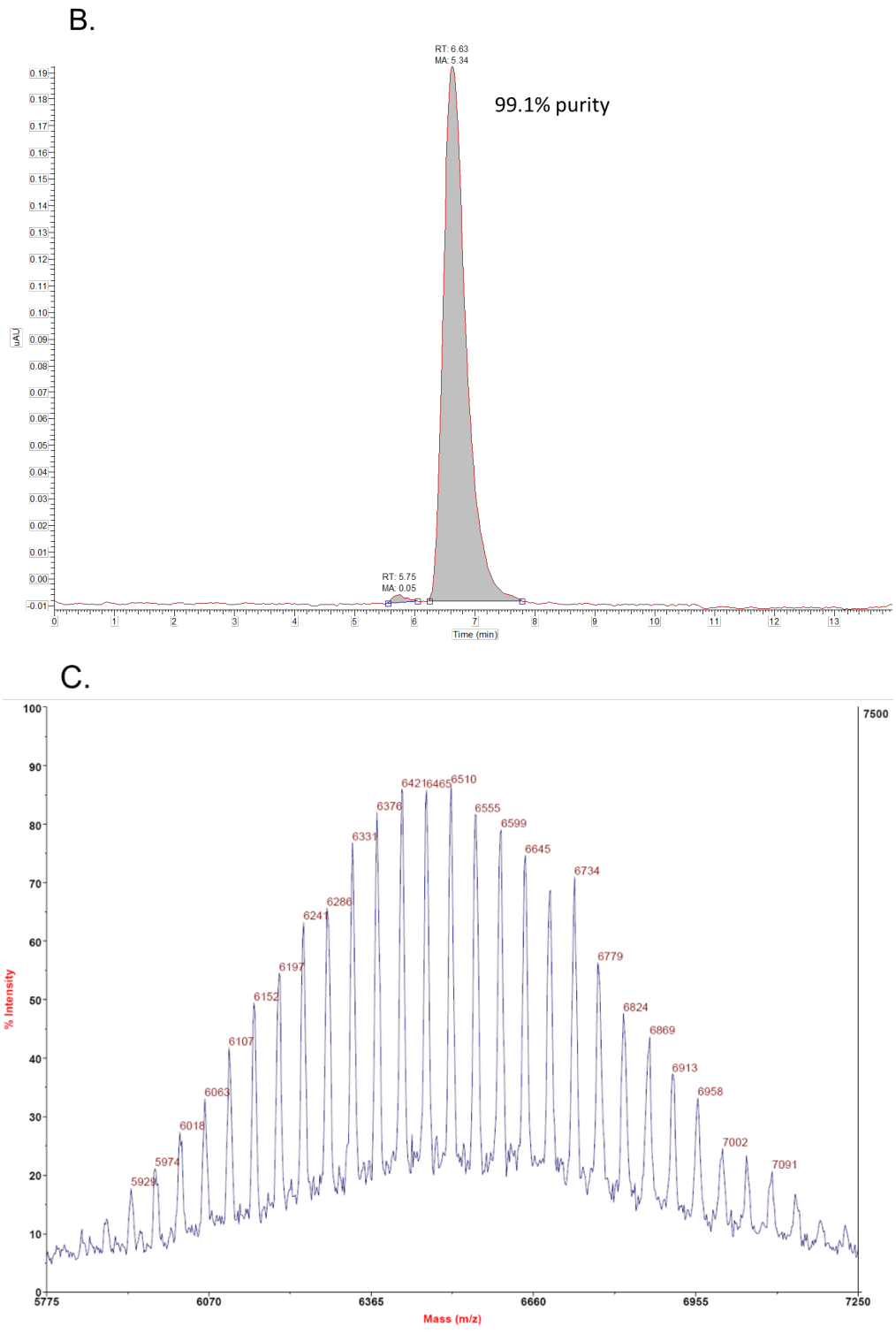

Figure S1. AVB-620 synthesis and purification. (A) Scheme for AVB-620 synthesis. **(B)** HPLC chromatogram of purified AVB-620. **(C)** MALDI-TOF Mass spectrometry analysis of AVB-620.

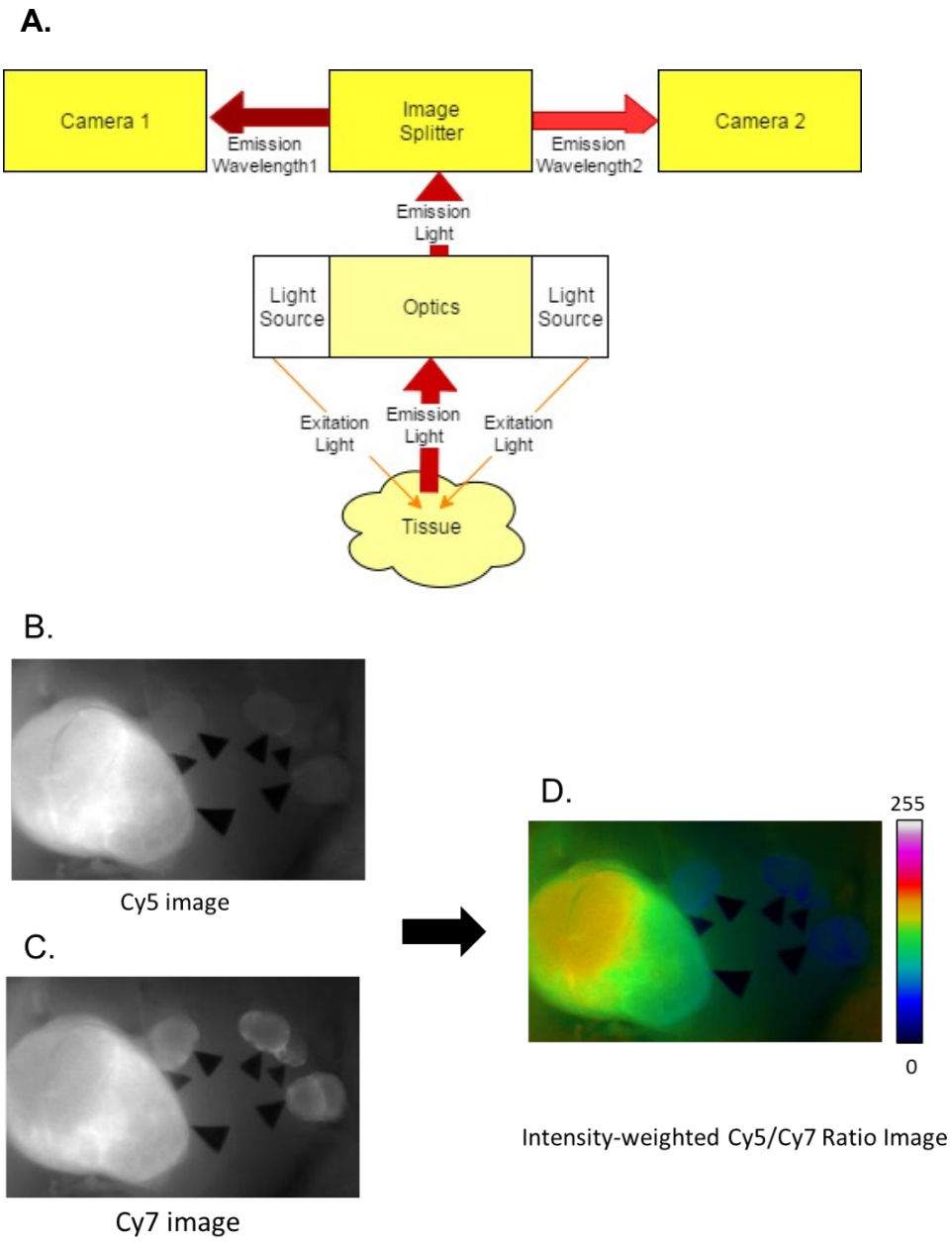

Figure S2. Generation of Cy5/Cy7 fluorescence ratio (FR) images example in 4T1 model. **(A)** Optical diagram of camera instrumentation used to capture FR images. **(B)** Cy5 fluorescence image (**C**) Cy7 fluorescence image and (**D**) Cy5/Cy7 FR image of cervical lymph nodes shown in Fig. 4C.

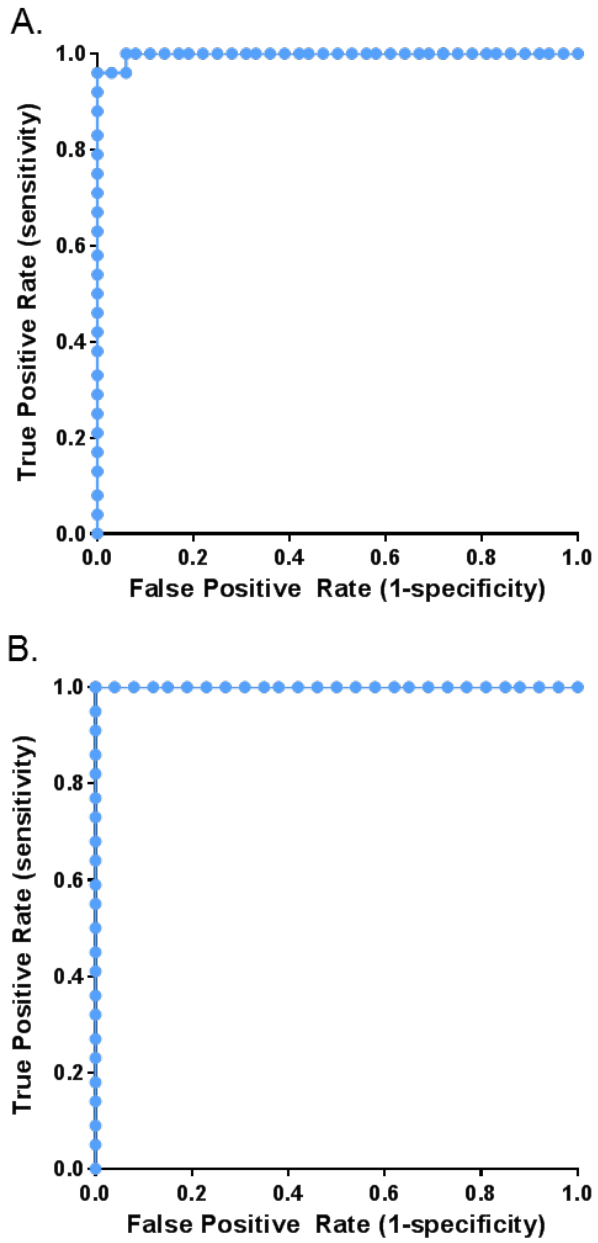

Figure S3. ROC curves for tumor metastasis imaging in lymph nodes. (A) 4T1 analysis using data from Fig. 4 **(B)** PyMT analysis using data from Fig. 5.

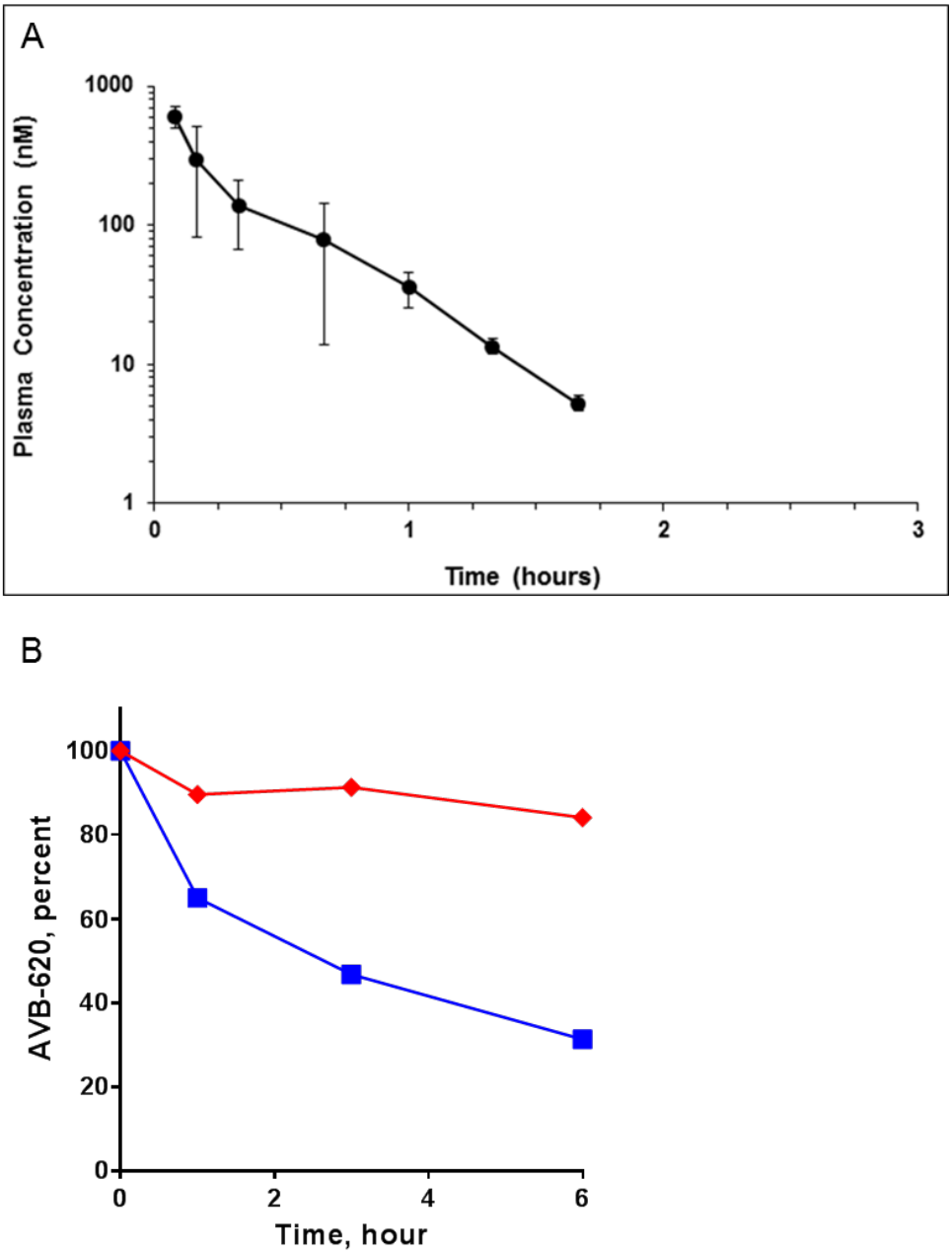

Figure S4. AVB-620 pharmacokinetics in mice and stability in plasma. (A) AVB-620 pharmacokinetics. BALB/c mice were injected IV with 1.7 mg/kg AVB-620 and then blood samples were taken from 5-100 minutes and assayed for AVB-620 after MeOH extraction using HPLC with fluorescent detection. Each data point represents the mean of 3-4 determinations and the error bars are standard deviation. (B) AVB-620 stability in human (red diamonds) and rat (blue squares) plasma. 10 µM AVB-620 was incubated at 37 °C in heparinized plasma. Samples were removed at time points, extracted and assayed by HPLC.

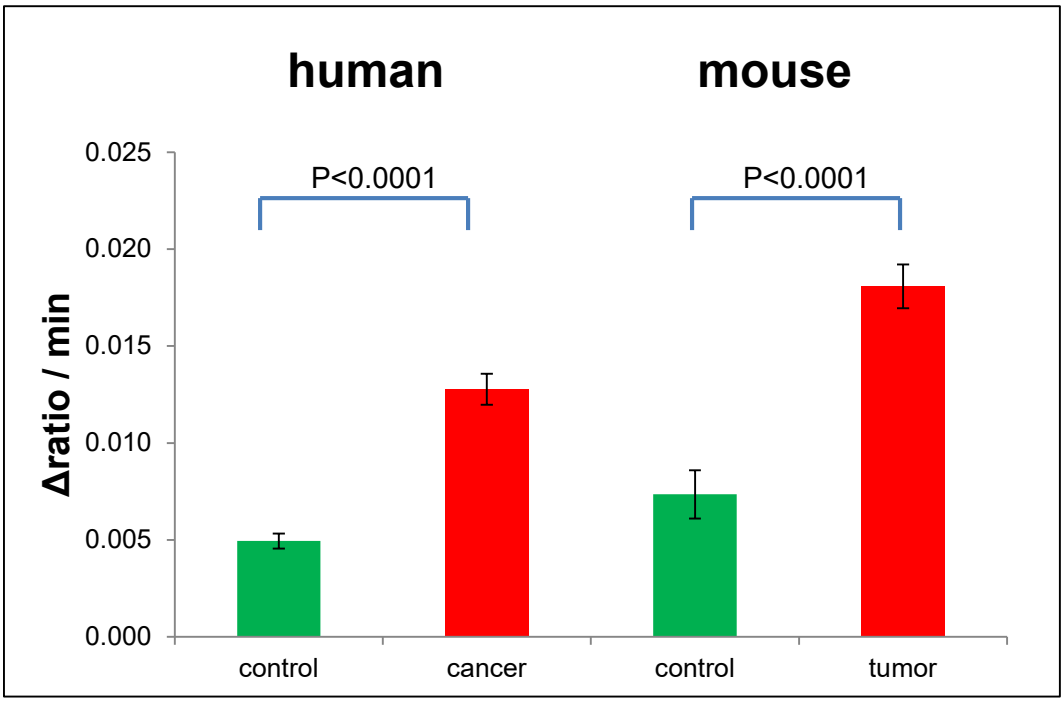

Figure S5. Comparison of AVB-620 hydrolysis rates in human and mouse tissue homogenates. Primary human tumor from breast cancer patients (n= 13) and uninvolved adjacent breast tissues (control), and murine 4T1 tumors (n= 8) and adjacent muscle tissues (control) were used. Values represent means ± standard error.